Surface Tension of the NaF + AlF_3 + $AlPO_4$ and NaF + AlF_3+ $NaVO_3$ Molten Systems

B. Kubíková,* Z. Tomášková, and J. Priščák

Institute of Inorganic Chemistry, Slovak Academy of Sciences, Dúbravská cesta 9, 845 36 Bratislava, Slovakia

Surface tensions of the parts of the NaF + AlF_3 + $AlPO_4$ and NaF + AlF_3 + $NaVO_3$ molten systems were investigated at four cryolite ratios (CR) [CR = n(NaF)/n(AlF_3)] varied between 1.5 and 3 (1.5, 2, 2.5, and 3). The maximum bubble pressure method was used for the determination of this physicochemical property. In general, small additions of $AlPO_4$ to the NaF−AlF_3 molten system cause a decrease of the surface tension. By melting $NaVO_3$ at low concentrations, new species with lower covalence of bonds occur compared with bonds of species presented in molten NaF−AlF_3.

Introduction

Aluminum is the most abundant metal in the Earth's crust and the third most abundant element therein, after oxygen and silicon. Aluminum is important for its ability to resist corrosion due to the passivation and for the metal's low density. Structural components made from aluminum and its alloys are essential in the aerospace industry and very important in other areas such as transportation and building. Its reactive nature makes it useful as a catalyst or additive in chemical mixtures, including being used in ammonium nitrate explosives to enhance blast power.

Aluminum is produced by the Hall−Héroult process where alumina is electrolyzed in a molten NaF−AlF_3 mixture. Industrial electrolytes contain impurities, like iron, silicon, sulfur, phosphorus, and vanadium.[1] The sources of these impurities are mainly alumina, fluoride compounds, and anodes.[2] Vanadium and phosphorus impurities cause a significant decrease of current efficiency in the aluminum cell.[3] Recently, the solubility of $AlPO_4$ and $NaVO_3$ in NaF + AlF_3 melts[4] and thermal analysis of the Na_3AlF_6 + $NaVO_3$ system[5] have already been determined. The authors performed the investigation at CR = 2 and 2.5 and found out that $AlPO_4$ decreases temperatures of primary crystallizations more compared with $NaVO_3$.[4] The study of thermal analysis of the system Na_3AlF_6 + $NaVO_3$ showed that the studied system is a simple eutectic one.[5]

Surface tension is one of the important parameters which affects the industrial electrolytic production of aluminum. Several interfaces are present in the aluminum electrolysis cell. The interfacial tension between the electrolyte and molten aluminum is connected especially with the dissolution rate of aluminum in the electrolyte. The interfacial tension between the carbon parts and the electrolyte affects the penetration of the electrolyte into the carbon lining. The surface tension of the molten bath influences the separation of the carbon particles from the electrolyte and the coalescence of the fine aluminum droplets.[2]

This paper is a contribution to the study of surface tension of two fluoride molten systems based on vanadium and phosphorus.

* Corresponding author. E-mail: uachkubi@savba.sk.

Experimental Section

For the preparation of samples, the following chemicals were used: AlF_3 sublimated in a platinum crucible, NaF (Merck, 99.9 %), $NaVO_3$ (Aldrich, anhydrous, 99.9 %), $AlPO_4$ (Aldrich, 99.99 %), and NaCl and KCl (all Fluka, p.a.). All chemicals were dried under vacuum at 150 °C for 5 h and handled in a glovebox under a dry nitrogen atmosphere (Messer, 99.99 %).

The surface tension of the NaF (1) + AlF_3 (2) + $AlPO_4$ (3) and NaF (1) + AlF_3 (2) + $NaVO_3$ (3) melts was determined using the maximum bubble pressure method.

The surface tension may be calculated according to eq 1

$$\gamma = \frac{r}{2}(P_{\max} - gh\rho) \tag{1}$$

where r/m is the capillary radius; P_{max}/Pa is the maximum bubble pressure when the bubble is a hemisphere with the radius equal to the radius of the capillary; g/m·s^{-2} is the acceleration of free fall; h/m is the depth of immersion of the capillary; and ρ/kg·m^{-3} is the density of the melt. However, there is also the possibility to calculate the surface tension of the liquid without knowing the density of the melt. Eliminating the density, ρ, from eq 1 for two different immersion depths we obtain the equation

$$\gamma = \frac{r}{2}\frac{P_{\max,1}h_2 - P_{\max,2}h_1}{h_2 - h_1} \tag{2}$$

where $P_{max,i}$ is the maximum bubble pressure at immersion depth h_i. Although the density data for the investigated melts were known, eq 2 was preferably used for the investigated melts. The surface tension of each sample was measured at four to six different temperatures in the range of (80 to 100) °C starting approximately 20 °C above the temperature of primary crystallization (t_m). The surface tension measurements were performed at four different depths of immersion (usually (2, 3, 4, and 5) mm) yielding six surface tension values for each temperature. A detailed description of the measuring procedure with experimental device can be found in another published work.[6]

10.1021/je901079k
Published on Web 08/17/2010

Table 1. Regression Coefficients *a* and *b* of the Temperature Dependence of the Surface Tension and the Standard Deviation of Mean (s_γ) of Individual Melts of the NaF (1) + AlF_3 (2) + $AlPO_4$ (3) System

	x_1	x_2	x_3	a / (mN·m^{-1})	b / (mN·m^{-1}·°C)	s_γ / (mN·m^{-1})	t / °C
CR = 3	0.7500	0.2500	0.0000	274.61	0.1383	0.29	1029 to 1097
	0.7425	0.2475	0.0100	277.48	0.1425	0.55	1029 to 1097
	0.7350	0.2450	0.0200	271.17	0.1383	0.67	1013 to 1099
	0.7275	0.2425	0.0300	263.47	0.1313	0.49	1018 to 1097
	0.7125	0.2375	0.0500	250.16	0.1176	0.73	995 to 1074
CR = 2.5	0.7143	0.2857	0.0000	272.49	0.1476	0.26	1024 to 1095
	0.7072	0.2828	0.0100	177.46	0.0582	0.60	1024 to 1133
	0.7000	0.2800	0.0200	184.94	0.0655	0.28	1003 to 1111
	0.6929	0.2771	0.0300	192.48	0.0739	0.54	1003 to 1085
	0.6786	0.2714	0.0500	182.67	0.0670	0.36	975 to 1022
CR = 2	0.6667	0.3333	0.0000	171.94	0.0659	0.39	981 to 1074
	0.6600	0.3300	0.0100	171.7	0.0665	0.14	983 to 1071
	0.6534	0.3266	0.0200	163.14	0.0591	0.39	985 to 1080
	0.6467	0.3233	0.0300	146.87	0.0434	0.24	924 to 1053
	0.6334	0.3166	0.0500	170.36	0.0679	0.08	960 to 1019
CR = 1.5	0.6000	0.4000	0.0000	164.03	0.0840	0.15	857 to 967
	0.5940	0.3960	0.0100	119.20	0.0325	0.08	875 to 952
	0.5880	0.3920	0.0200	118.83	0.0330	0.37	838 to 948
	0.5820	0.3880	0.0300	128.67	0.0446	0.28	807 to 908
	0.5700	0.3800	0.0500	133.34	0.0480	0.35	777 to 870

Table 2. Regression Coefficients *a* and *b* of the Temperature Dependence of the Surface Tension and the Standard Deviation of Approximation (s_γ) of Individual Melts of the NaF (1) + AlF_3 (2) + $NaVO_3$ (3) System

	x_1	x_2	x_3	a / (mN·m^{-1})	b / (mN·m^{-1}·°C)	s_γ / (mN·m^{-1})	t / °C
CR = 3	0.7500	0.2500	0.0000	274.61	0.1383	0.29	1029 to 1097
	0.7425	0.2475	0.0100	294.63	0.1555	0.41	1024 to 1107
	0.7350	0.2450	0.0200	267.85	0.1291	0.71	1025 to 1116
	0.7275	0.2425	0.0300	295.11	0.1552	0.42	1022 to 1101
	0.7125	0.2375	0.0500	286.17	0.1486	0.14	1024 to 1105
CR = 2.5	0.7143	0.2857	0.0000	272.49	0.1476	0.26	1024 to 1095
	0.7072	0.2828	0.0100	283.78	0.1551	0.20	1011 to 1079
	0.7000	0.2800	0.0200	311.98	0.1820	0.27	1010 to 1085
	0.6929	0.2771	0.0300	277.78	0.1499	0.19	1004 to 1060
	0.6786	0.2714	0.0500	305.81	0.1805	0.15	996 to 1054
CR = 2	0.6667	0.3333	0.0000	171.94	0.0659	0.39	1001 to 1067
	0.6600	0.3300	0.0100	306.79	0.2005	1.13	973 to 1024
	0.6534	0.3266	0.0200	313.33	0.2074	0.35	975 to 1033
	0.6467	0.3233	0.0300	247.34	0.1393	0.46	964 to 1020
	0.6400	0.3200	0.0400	236.36	0.1278	0.17	963 to 1018
CR = 1.5	0.6000	0.4000	0.0000	164.03	0.0840	0.15	857 to 967
	0.5880	0.3920	0.0200	225.91	0.1593	0.13	830 to 885
	0.5820	0.3880	0.0300	214.07	0.146	0.12	830 to 882
	0.5700	0.3800	0.0500	227.75	0.1554	0.37	831 to 878

In the surface tension measurements using the maximum bubble pressure method, several sources of error may occur. As mentioned above, the exact machining of the capillary orifice is important. A deviation from a circular orifice caused in our case an error of ± 0.5 %. The determination of the immersion depth with a precision of ± 0.01 mm introduced an error of ± 0.5 %. The precision of ± 1 Pa in the pressure measurement caused an additional error of ± 0.5 %. The sum of all these errors gives an estimated total error of approximately ± 1.5 %. The standard deviations of the experimental data, based on the least-squares statistical analysis, were in the range of (0.08 to 1.13) mN·m^{-1} which corresponds to the estimated error. The uncertainty of temperature measurement u_t was u_t = 2 °C.

The temperature dependence of the surface tension of particular mixtures was expressed by the linear equation

$$\gamma = a - bt \tag{3}$$

where γ/mN·m^{-1} is the surface tension and t/°C is the temperature. The values of the constants a/mN·m^{-1} and b/mN·m^{-1}·°C in eq 3, obtained from the linear regression analysis, together with the values of the standard deviations of the mean (s_γ/mN·m^{-1}), for the investigated NaF (1) + AlF_3 (2) + $AlPO_4$ (3) and NaF (1) + AlF_3 (2) + $NaVO_3$ (3) melts are given in Table 1 and Table 2, respectively.

Results and Discussion

The concentration dependences of the surface tension of the NaF (1) + AlF_3 (2) + $AlPO_4$ (3) molten system at four cryolite ratios (CR = 1.5, 2, 2.5, and 3) at three chosen temperatures are shown in Figures 1 to 4. The presented temperatures were selected in order to cover the real temperature range of investigation. At all selected temperatures are samples in molten state. The same reason is valid also for the second investigated system.

The surface tension of the NaF (1) + AlF_3 (2) + $AlPO_4$ (3) molten system at CR = 1.5 for three temperatures (t = (820, 830, and 840) °C) is shown in Figure 1. At the beginning, surface tension rapidly decreases with increasing content of $AlPO_4$ (3) in the NaF (1) + AlF_3 (2) system. Then, the lowest value reaches surface tension at x_3 = 0.02, and subsequently the surface tension increases with further addition of $AlPO_4$ (3) to the NaF (1) + AlF_3 (2) system.

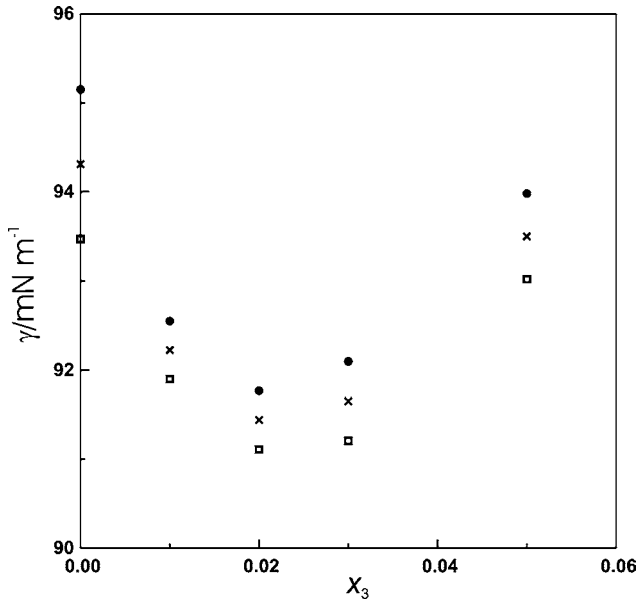

Figure 1. Surface tension of the NaF (1) + AlF_3 (2) + $AlPO_4$ (3) system at CR = 1.5: ●, 820 °C; ×, 830 °C; □, 840 °C.

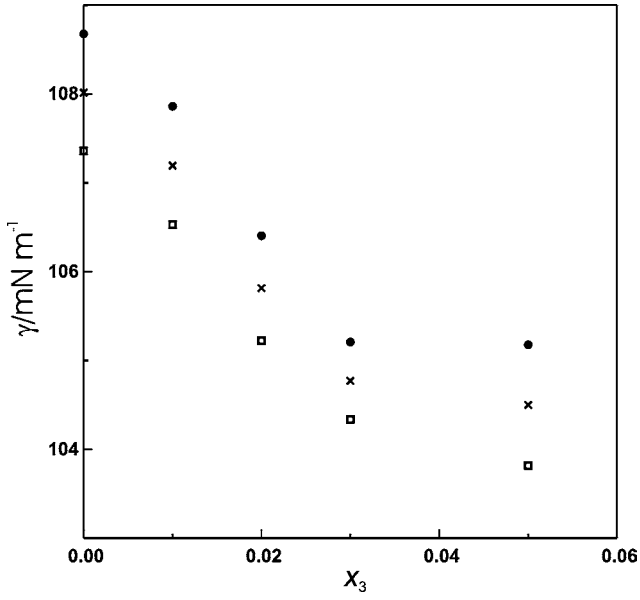

Figure 2. Surface tension of the NaF (1) + AlF_3 (2) + $AlPO_4$ (3) system at CR = 2: ●, 960 °C; ×, 970 °C; □, 980 °C.

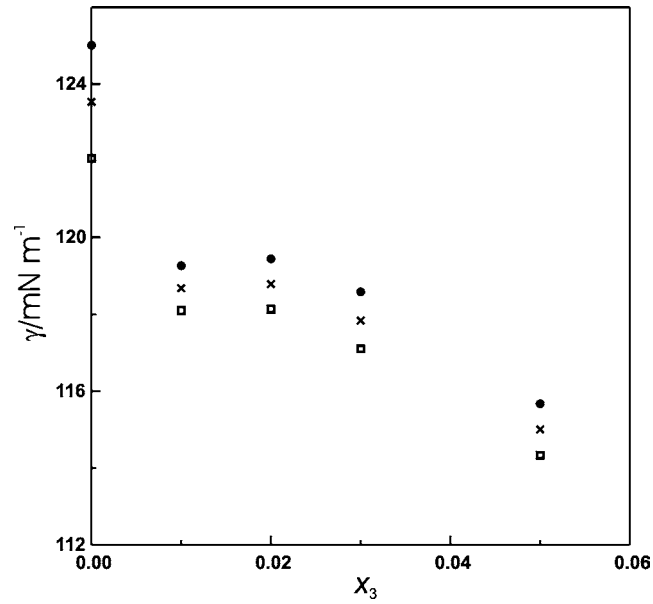

Figure 3. Surface tension of the NaF (1) + AlF_3 (2) + $AlPO_4$ (3) system at CR = 2.5: ●, 1000 °C; ×, 1010 °C; □, 1020 °C.

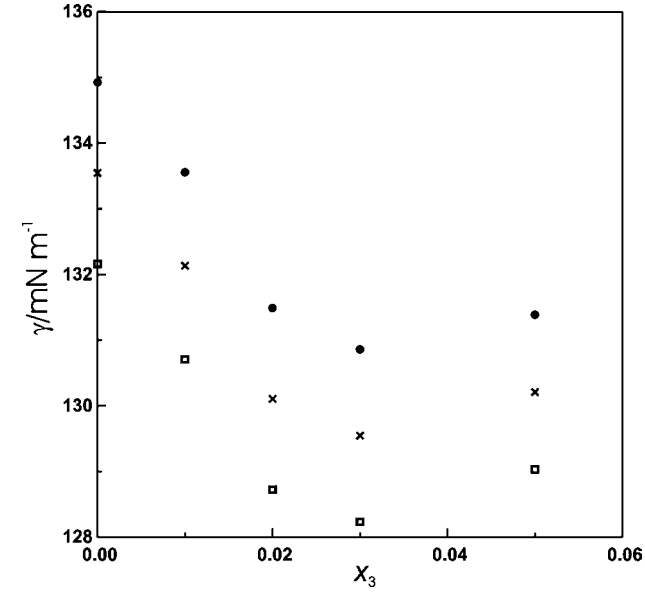

Figure 4. Surface tension of the NaF (1) + AlF_3 (2) + $AlPO_4$ (3) system at CR = 3: ●, 1010 °C; ×, 1020 °C; □, 1030 °C.

Figure 2 shows the concentration dependence of surface tension in the molten NaF (1) + AlF_3 (2) + $AlPO_4$ (3) system at CR = 2 for three selected temperatutes (t = (960, 970, and 980) °C). The surface tension of the investigated systems decreases in the whole studied concentration range with increasing content of $AlPO_4$ (3) to the NaF (1) + AlF_3 (2) system.

The surface tension of the NaF (1) + AlF_3 (2) + $AlPO_4$ (3) molten system at CR = 2.5 decreases with increasing content of $AlPO_4$ (3) for all three chosen temperatures (t = (1000, 1010, and 1020) °C). A small divergence occurs at $x_3 = 0.02$, where surface tension slowly increases.

The behavior of concentration dependence of surface tension in the NaF (1) + AlF_3 (2) + $AlPO_4$ (3) molten system at CR = 3 (Figure 4) is similar to the concentration dependence of surface tension in the NaF (1) + AlF_3 (2) + $AlPO_4$ (3) molten system at CR = 2 (Figure 2). The surface tension decreases with increasing content of $AlPO_4$ (3). At $x_3 = 0.05$, surface tension slowly increases.

In general, small additions of $AlPO_4$ (3) to the NaF (1) + AlF_3 (2) system causes decreasing of the surface tension, which means that $AlPO_4$ (3) is a surface active component in NaF (1) + AlF_3 (2).

The concentration dependences of the surface tension of the NaF (1) + AlF_3 (2) + $NaVO_3$ (3) molten system at four cryolite ratios (CR = 1.5, 2, 2.5, and 3) at three selected temperatures are shown in Figures 5 to 8.

From Figure 5, it is evident that surface tension decreases with the addition of $NaVO_3$ (3) to the molten NaF (1) + AlF_3 (2) system at CR = 1.5, and subsequently, the surface tension rapidly increases with increasing content of $NaVO_3$ (3). This movement is typical for all three chosen temperatures t = (820, 830, and 840) °C.

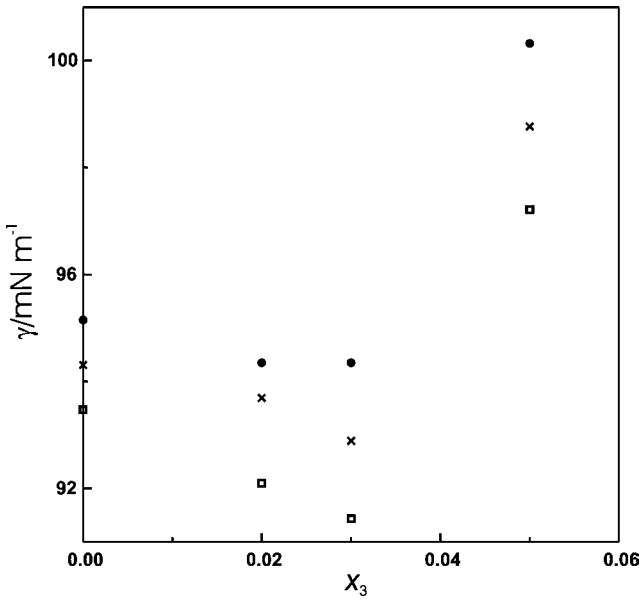

Figure 5. Surface tension of the NaF (1) + AlF_3 (2) + $NaVO_3$ (3) system at CR = 1.5: ●, 820 °C; ×, 830 °C; □, 840 °C.

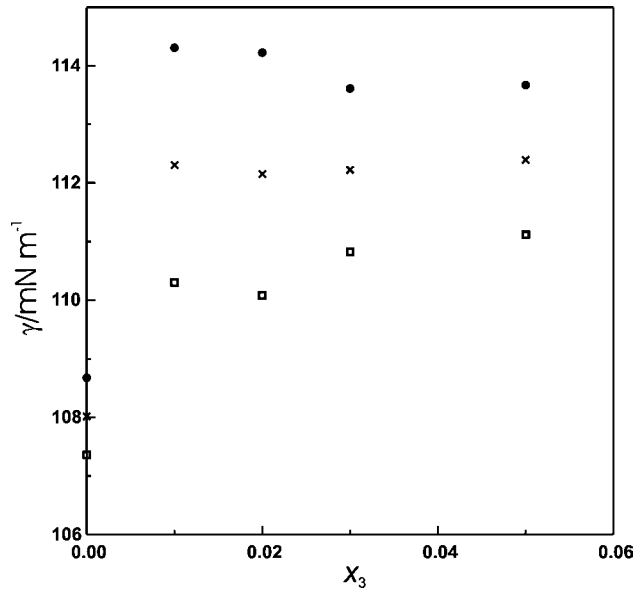

Figure 6. Surface tension of the NaF (1) + AlF_3 (2) + $NaVO_3$ (3) system at CR = 2: ●, 960 °C; ×, 970 °C; □, 980 °C.

The surface tension rapidly increases with the addition of $NaVO_3$ (3) to the molten NaF (1) + AlF_3 (2) system at CR = 2 for all three temperatures (t = (960, 970, and 980) °C) (Figure 6). Further addition of $NaVO_3$ (3) to the NaF (1) + AlF_3 (2) system at CR = 2 did not cause strong changes in values of surface tension, and it reached almost constant values.

Figure 7 represents the concentration dependence of surface tension in the NaF (1) + AlF_3 (2) + $NaVO_3$ (3) molten system at temperatures t = (1000, 1010, and 1020) °C and CR = 2.5. The surface tension of the NaF (1) + AlF_3 (2) + $NaVO_3$ (3) increases with low content of $NaVO_3$ (3) and reaches a maximum at $x_3 = 0.02$, and subsequently, the surface tension slowly decreases. It is evident that by melting of $NaVO_3$ (3) at low concentrations a new species with lower covalence of bonds occurs compared with bonds of species presented in molten NaF (1) + AlF_3 (2).

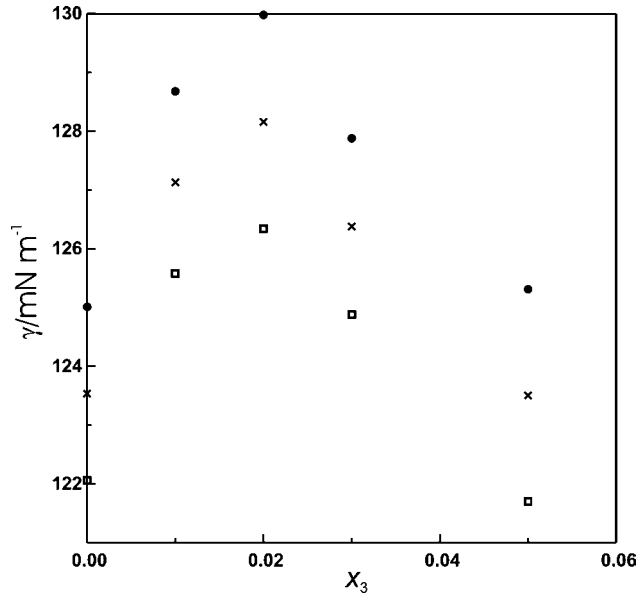

Figure 7. Surface tension of the NaF (1) + AlF_3 (2) + $NaVO_3$ (3) system at CR = 2.5: ●, 1000 °C; ×, 1010 °C; □, 1020 °C.

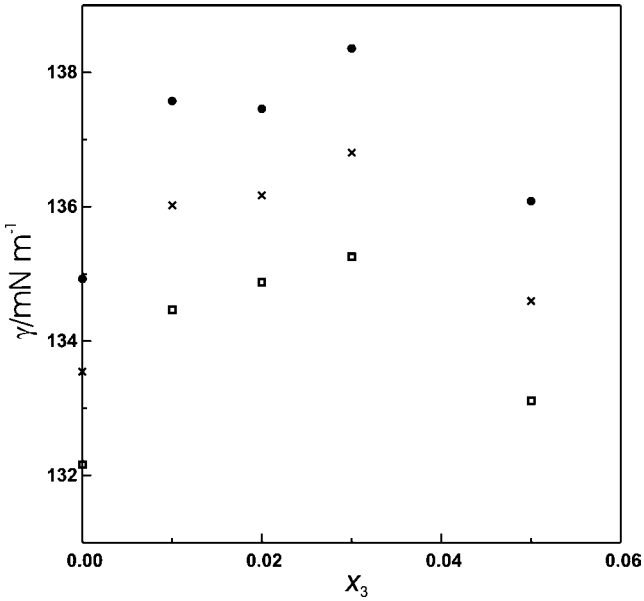

Figure 8. Surface tension of the NaF (1) + AlF_3 (2) + $NaVO_3$ (3) system at CR = 3: ●, 1010 °C; ×, 1020 °C; □, 1030 °C.

A similar result is typical also for the concentration dependence of the NaF (1) + AlF_3 (2) + $NaVO_3$ (3) molten system at temperatures t = (1010, 1020, and 1030) °C and CR = 3 (Figure 8). With the first addition of $NaVO_3$ (3) to the NaF (1) + AlF_3 (2), the surface tension increases. Then, surface tension slowly decreases with the increasing content of $NaVO_3$ (3), and the maximum is reached at $x_3 = 0.03$.

Supporting Information Available:

Temperature dependences (T) of surface tension (γ) for four cryolite ratios (CR) for both investigated systems. This material is available free of charge via the Internet at http://pubs.acs.org.

Literature Cited

(1) Grjotheim, K.; Krohn, C.; Malinovský, M.; Matiašovsky, K.; Thonstad, J. *Aluminium Electrolysis, Fundamentals of the Hall—Héroult Process*, 2nd ed.; Aluminium-Verlag: Düsseldorf, 1982.

(2) Thonstad, J.; Fellner, P.; Haarberg, G. M.; Híveš, J.; Kvande, H.; Sterten, Å. *Aluminium Electrolysis, Fundamentals of the Hall—Héroult Process*, 3rd ed.; Aluminium-Verlag: Düsseldorf, 2001.
(3) Sterten, Å.; Solli, P. A.; Skybakmoen, E. Influence of electrolyte impurities on current efficiency in aluminium electrolysis cells. *J. Appl. Electrochem.* **1998**, *28*, 781–789.
(4) Kucharík, M.; Vasiljev, R. Solubility of $AlPO_4$ and $NaVO_3$ in NaF-AlF_3 melts. *J. Chem. Eng. Data* **2008**, *53*, 1817–1819.
(5) Kucharík, M.; šimko, F.; Danielik, V.; Boča, M.; Vasiljev, R. Thermal analysis of the system Na_3AlF_6—$NaVO_3$. *Monatsh. Chem.* **2007**, *138*, 1211–1215.
(6) Kucharík, M.; Vasiljev, R. Surface Tension of the System NaF—AlF_3—Al_2O_3 and Surface Adsorption of Al_2O_3. *Z. Naturforsch.* **2006**, *61a*, 389–398.

Received for review January 13, 2010. Accepted July 23, 2010. The Slovak Grant Agencies APVV LPP-0345-09 and VEGA 2/7077/27 and 2/0058/09 are acknowledged for financial support.

JE901079K